



HAL
open science

Estimating and restoring bedload transport through a run-of-river reservoir

T. Depret, H. Piegay, V. Dugué, L. Vaudor, J.B. Faure, Jérôme Le Coz, B. Camenen

► **To cite this version:**

T. Depret, H. Piegay, V. Dugué, L. Vaudor, J.B. Faure, et al.. Estimating and restoring bedload transport through a run-of-river reservoir. *Science of the Total Environment*, Elsevier, 2019, 654, pp.1146-1157. 10.1016/j.scitotenv.2018.11.177 . hal-02608072

HAL Id: hal-02608072

<https://hal.inrae.fr/hal-02608072>

Submitted on 16 May 2020

HAL is a multi-disciplinary open access archive for the deposit and dissemination of scientific research documents, whether they are published or not. The documents may come from teaching and research institutions in France or abroad, or from public or private research centers.

L'archive ouverte pluridisciplinaire **HAL**, est destinée au dépôt et à la diffusion de documents scientifiques de niveau recherche, publiés ou non, émanant des établissements d'enseignement et de recherche français ou étrangers, des laboratoires publics ou privés.

Estimating and restoring bedload transport through a run-of-river reservoir

Thomas Dépret^{a,b*}, Hervé Piégay^a, Violaine Dugué^{c,d}, Lise Vaudor^a,
Jean-Baptiste Faure^c, Jérôme Le Coz^c, Benoît Camenen^c

^a Université de Lyon, CNRS, UMR 5600 - Environnement-Ville-Société, Site ENS de Lyon, 15 Parvis
René Descartes, Lyon 69342, France

^b now Laboratoire de Géographie Physique, CNRS UMR8591, 1 Place Aristide Briand, 92195
Meudon, France

^c Irstea, UR RiverLy, centre de Lyon-Villeurbanne, 5 Rue de la Doua, CS 20244, F-69625
Villeurbanne Cedex, France

^d now Compagnie Nationale du Rhône, 2 rue André Bonin, 69004 Lyon, France

* Corresponding author, e-mail address: thomas.depret@lgp.cnrs.fr

Abstract

Weirs or run-of-river dams can disrupt bedload transfer with negative ecological effects downstream due to sediment starvation. The way and the degree to which bedload is trapped is nevertheless not straightforward and few studies have examined this topic. This study focuses on a 13-km-long reservoir of the Rhône River, France, created by a diversion dam equipped with bottom gates. Our main objective was to determine the degree of alteration of the bedload transfer downstream and to identify to which extent the implementation of Ecomorphogenic Flow (EmF), defined as environmental flow whose objective is specifically to increase bedload transfer through the reservoir to promote downstream habitat diversity, could increase bed mobility. The results show that the potential for morphological adjustments in the reservoir was already low before dam completion (1968) in response to a substantial decrease in coarse sediment supply, but that this potential was progressively reduced due to the impoundment. However, the bedload transfer continuity has been at least partially maintained since dam completion. According to numerical simulations, only particles smaller than medium gravels ($d < 14$ mm) could be exported downstream of the dam for relatively rare discharge (50-years return-interval flood). Implementation of EmF could neatly improve the bedload transfer since it would allow to strongly increase the competence: for a 2-years and a 50-years return-interval floods, the maximum particle size exportable downstream is respectively 9 and 4 times larger than for normal functioning of the reservoir operating.

38 **Keywords**

39 Environmental flow; Bedload continuity; Flow competence; Process-based restoration; Run-of-river
40 dam; Impoundment

41

42 **Highlights**

43 - Partial maintenance of bedload transfer through a run-of-river reservoir of a large gravel-bed
44 river

45 - Integrated approach combining sediment budgets and hydraulic modelling

46 - Increase of bed mobility through implementation of Environmental Flows

47

48

49 **1. Introduction**

50 The effects of large dams on river morphology and sediment transport have been widely studied
51 and are therefore relatively well known. Since they modify the upstream hydraulic condition in the
52 impounded sections by lowering the energy slope, dams interrupt bedload transport and sometimes
53 suspended load, inducing a progressive filling of the reservoirs (Kondolf et al., 2014; Morris et al.,
54 2008). Whereas at their entrance, coarse sediment deposits form a prograding delta with grain size
55 decreasing with downstream distance, reservoirs are mainly filled by fine and more homogenous silty
56 deposits that can be settled by turbidity currents (Kostic and Parker, 2003; Lajczak, 1996; Morris and
57 Fan, 1998; Snyder et al., 2004). Downstream of dams, the effects of flow and sediment regime
58 alteration is highly variable, depending on the pre-dam context (sediment size and supply, competence
59 and capacity of the river, flow regime) and on the intensity and nature of the perturbations (Williams
60 and Wolman, 1984; Brandt, 2000; Petts and Gurnell, 2005, 2013; Schmidt and Wilcock, 2008; Curtis
61 et al., 2010; Dade et al., 2011; Grant, 2012). Most of the time, dams cause a geomorphic simplification
62 (Graf, 2006), generally induced by bed incision, a decrease in lateral mobility and bed armouring
63 (Rollet et al., 2013). Together with the modification of the flow regime, geomorphic simplification
64 results in a loss in aquatic and riparian ecological diversity (Lobrerera et al., 2016; Nilsson and
65 Berggren, 2000; Rolls and Bond, 2017; Rosenberg et al., 2000).

66 Until very recently, less attention has been paid to the impacts of run-of-river dams (Csiki and
67 Rhoads, 2010, 2014; Ibisate et al. 2013), despite their widespread presence. Yet, particularly because
68 of their potential cumulative effects, series of run-of-river dams can also modify hydrological and
69 sediment dynamics, as well as ecological functions (Dessaix et al., 1995; Kibler and Tullus, 2013;
70 Anderson et al., 2015; Fencl et al., 2015). The term “run-of-river dam” still suffers from a lack of a
71 clear definition, and other words such as “weir”, “low-head dam”, “overflow dam” or “small dam” are
72 usually employed to define similar kinds of structures (Csiki and Rhoads, 2010, 2014; Fencl et al.,
73 2015). Here, we will retain the definition given by Csiki and Rhoads (2010), namely a “structure that
74 extends across the width of a stream or river channel, has no mechanism inhibiting discharge of water

75 over the dam, and is of a height that generally does not exceed the elevation of the channel banks
76 upstream – i.e., water stored upstream at base flow is contained within the river channel width of a
77 stream or river channel”. Costigan et al. (2016) note that 97% of dams in the United States are run-of-
78 river dams. In France, the ROE (Référentiel des Obstacles à l’Ecoulement), a large national database
79 listing most of the transverse engineering structures impeding flow, identifies more than 57,400 weirs
80 (May 2014 inventory), namely 81% of the total number of dams. Concerning their influence on
81 bedload, two main questions systematically arise. First, how much is the sediment transport altered?
82 Second, in case of partial or total interruption, what solutions could be applied to enhance or restore
83 the sediment transfer through the reservoir? In some countries of the European Union, this concern has
84 been integrated into the national legislative frame following the Water Framework Directive. In
85 France for example, authorities must now guarantee “sufficient transport” maintaining or restoring the
86 morphological and ecological structures and functions of rivers (Malavoi et al., 2011).

87 All other conditions being equal, the intensity of a run-of-river dam’s influence on the
88 morphodynamics and coarse sediment transport in impounded reaches is mainly controlled by the
89 presence or absence of bottom gates. In absence of such gates or when they are maintained closed, and
90 at least in an initial stage, all or most of the bedload can be trapped in the reservoir (Kibler et al., 2011;
91 Pearson and Pizzuto, 2015) and the grain size of coarse deposits tends to show a decreasing
92 downstream pattern (Sindelar et al., 2017). Depending on dam height, bed hydraulic characteristics
93 before impoundment, grain size and sediment yield, bedload transfer can nevertheless be preserved or
94 restored, at least for medium-term periods. For example, Csiki and Rhoads (2014) documented the
95 case of four run-of-river dams showing an absence of a statistically significant difference in the
96 percentage of sand or gravel in the bed material between upstream and downstream portions of dams,
97 indicating no coarse sediment accumulation in the reservoir and a probable preservation of the bedload
98 transfer continuity. Pearson and Pizzuto (2015) demonstrated that partial reservoir filling can be
99 sufficient to reestablish sediment transfer if a gently sloping ramp is formed just upstream of the dam.
100 If the bedload transfer is disrupted too much, and if there are no possibilities to control water level or
101 discharge, dam removal is the only option for restoring continuity (Bednarek, 2001; Magilligan et al.,
102 2016).

103 The presence of bottom gates should theoretically reduce the dam’s influence on bedload, and so
104 should maintain, at least partially, sediment transfer. This is, for example, the case of the Jons dam on
105 the Rhône River (France), where opening the gates for a discharge slightly lower than the annual flood
106 allows the entire bedload to pass (Petit et al., 1996). If needed, the sediment transfer can be enhanced
107 through flushing and/or sluicing operations whose effects can be reinforced using different strategies,
108 implying a modification of the functioning of the plant associated with the dam, or construction of
109 engineering works along the reservoir, such as training walls (Bieri et al., 2012; Bizzi et al., 2015;
110 Isaac and Eldho, 2016; Sindelar et al., 2017).

111 When bedload transfer aims at being restored for ecological considerations, water releases can be
112 implemented as part of environmental flows (Poff, 2017; Poff et al., 2017; Poff and Zimmerman,
113 2010), defined in the Brisbane declaration (2007) as “the quantity, timing, and quality of the water
114 flows required to sustain freshwater and estuarine ecosystems and the human livelihoods and well-
115 being that depend on them” (<http://www.watercentre.org/news/declaration>). If the objective of such
116 operation is specifically to increase bedload transfer to promote downstream habitat diversity, we
117 suggest using the term “Ecomorphogenic Flows” (EmF). An increase in bedload transport is supposed
118 to promote local sediment storage such as bars which should create topographic and grain size
119 variability that will provide a variety of habitats for organisms (Gaeuman, 2012; Yarnell et al., 2006),
120 a higher range of hydraulic patterns and an improved connectivity between benthic and hyporheic
121 compartments. While such process-based restoration is highly attractive, especially because of its
122 expected long-lasting and sustainable effects (Beechie et al., 2010), it can nevertheless be difficult to
123 implement depending on the context because of the frequent need for trade-off with other water uses
124 such as navigation, electricity production and irrigation. An alternative to this solution can be coarse
125 sediment augmentation downstream of dams (Arnaud et al., 2017; Gaeuman, 2012; Rheinheimer and
126 Yarnell, 2017).

127 The main objectives of this paper are to provide answers to the following questions. How much can
128 a river bed readjust in a run-of-river reservoir following dam completion? What are the current
129 conditions of bed-material load entrainment in the reservoir? What is the degree of bedload transfer
130 downstream of the reservoir? Could bedload mobilization be improved for mitigating downstream
131 ecological impacts? What are the consequences of these issues for bedload management and
132 restoration? We focus on a case study, the Bourg-lès-Valence reach (Figure 1), which can serve as a
133 reference frame for the coarse sediment management of most of the other reservoirs of the Rhône
134 River (France) and more broadly of rivers influenced by run-of-river dams and presenting a strong and
135 long-standing bedload deficit.

136
137

138 2. Study site

139 2.1. Rhône River context

140 Coming from the Swiss Alps, the Rhône River flows over 812 km draining a catchment area of
141 98,500 km² (512 km long, with 90,500 km² in France, cf. Figure 1; Olivier et al., 2009; Bravard,
142 2010). The runoff at its outlet accounts for one-sixth of the total runoff into the Mediterranean Sea
143 (Fruget and Dessaix, 2003).

144 During the second half of the 20th century, the Rhône River underwent an important phase of
145 taming with the construction of 16 artificial canals parallel to the river course (Stroffek et al., 1996;
146 Olivier et al., 2009; Bravard and Gaydou, 2015). These canals were built to convey most of the annual
147 runoff to hydropower plants, improve commercial navigation and increase irrigation (Stroffek et al.,

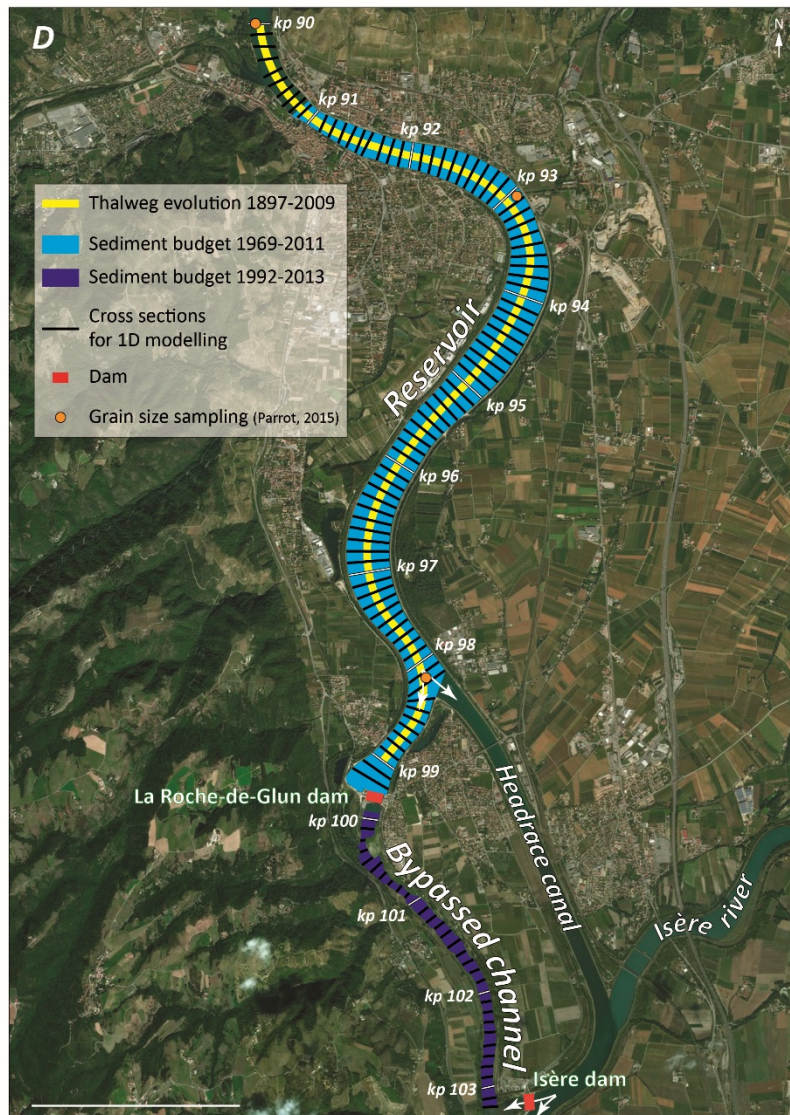
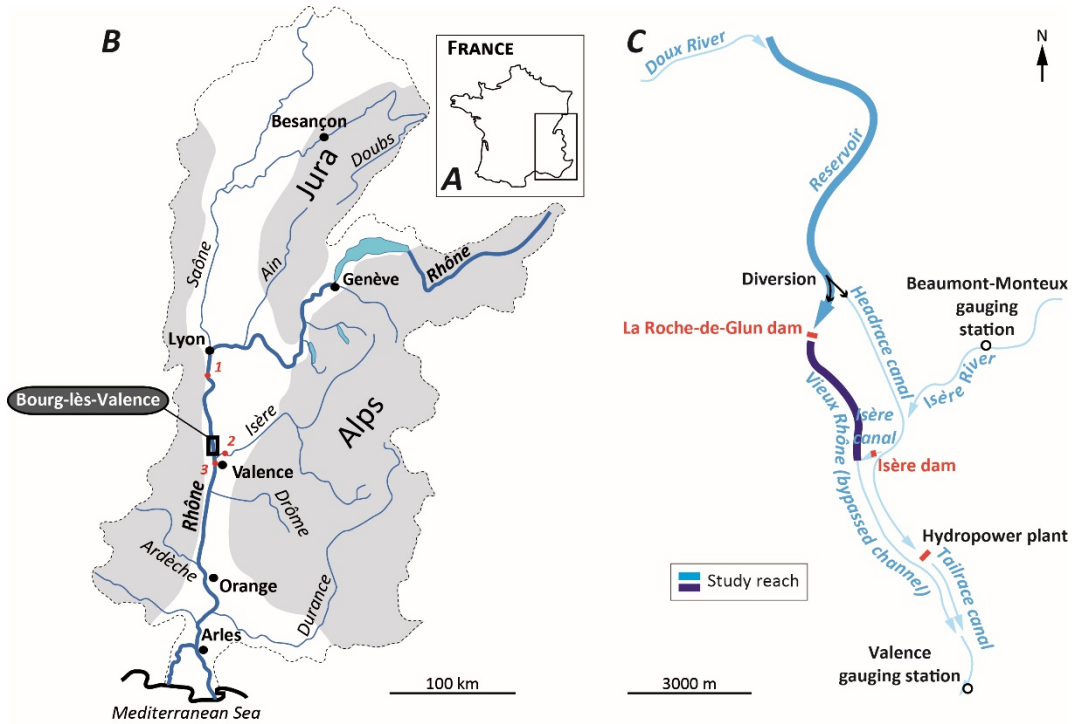
148 1996; Olivier et al., 2009; Bravard and Gaydou, 2015). Since then, the discharge in bypassed reaches
149 is residual (until 2014, between 1/3 and 1/322 of the average discharge), except during floods when
150 discharge is higher than the power plants capacity. The Rhône River is thus composed of a quasi-
151 continuous series of reservoirs and bypassed reaches. Located at the upstream end of the bypassed
152 reaches, diversion dams (run-of-river dams with diversion according to the classification of
153 McManamay et al., 2016) are equipped with bottom gates that are opened during high flows,
154 theoretically allowing the transport of coarse sediments. While bedload continuity remains possible,
155 dams have modified the condition of bedload transport through the reservoirs to an unknown extent.
156 Further, bedload could actually be null due to the low frequency for which critical shear stresses are
157 exceeded. The coarse sediment yield has indeed decreased since the second half of the 19th century due
158 to the channelization of the riverbed associated with bank protections downstream of Lyon (lateral
159 dykes, weirs, groynes, cross-beams) (Bravard, 1987; Bravard and Gaydou, 2015; Poinart, 1992;
160 Poinart and Salvador, 1993), preventing any sediment supply by lateral erosion. It is also affected by
161 a reduction in sediment supply from the tributaries (Astrade et al., 2011; Bravard, 2002; Bravard et al.,
162 1999; Bravard and Peiry, 1993; Lefort and Chapuis, 2012; Liébault et al., 1999, 2002; Liébault and
163 Piégay, 2002; Rollet et al., 2013; Warner, 2000). Due to channel incision, sediment winnowing and
164 sediment supply control, bedload is very low on most of the river course and the bed is armoured
165 (Cortier and Couvert, 2001). Nevertheless, respective impacts of each main taming phase on bedload
166 transport still need to be quantified and we do not know precisely if the bed is still able to adjust
167 vertically, since this dimension is the only one in which morphological changes can occur. To counter
168 the adverse effects of these two main taming phases, a large restoration project was initiated in the
169 1990s (Lamouroux et al., 2015) to improve main channel and former channel ecological diversity in
170 bypassed reaches. In a first step the minimal flow was increased and abandoned channels were
171 rejuvenated by dredging. More recently, a new strategy has emerged, more focused on process-based
172 restoration with riprap removal to reactivate bedload transport and shifting riverscape mosaics, raising
173 especially the question of the potential for bedload transfer through impounded reaches.

174

175 **2.2 Bourg-lès-Valence reach**

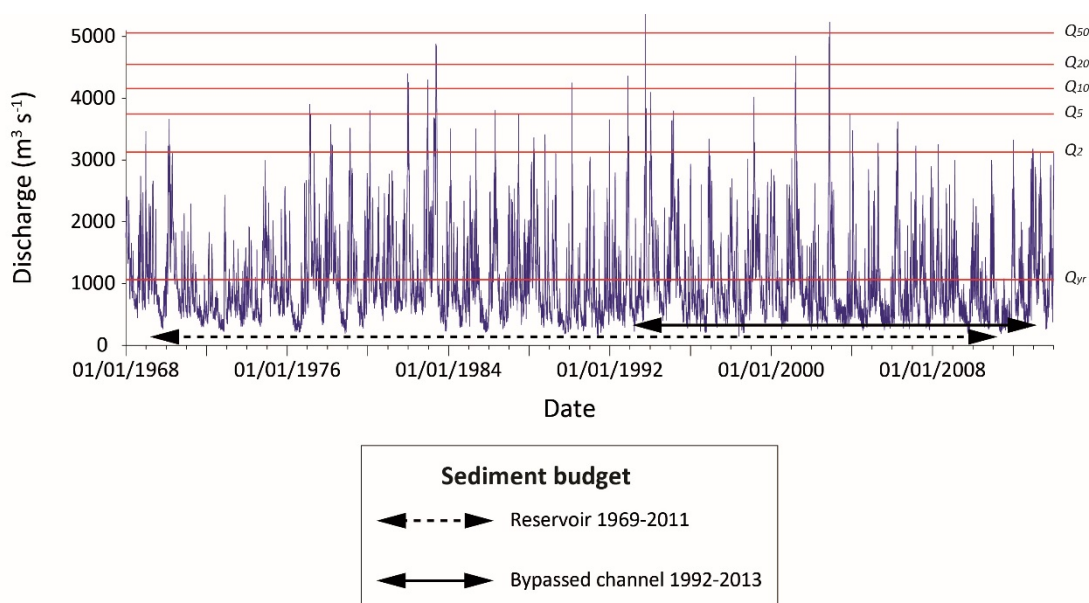
176 The study reach is located in the middle section of the Rhône River, just upstream of its confluence
177 with the Isère River, one of its most important tributaries (e.g., catchment size : 11,900 km²; mean
178 annual flow at the Beaumont-Montoux gauging station: 329 m³ s⁻¹) (Figure 1). In the same way as the
179 whole Rhône river course downstream of Lyon, the Rhône in this section was constricted from the
180 mid-19th century to the first part of the 20th century with engineering works, built in three steps.
181 Dikes in the floodplain were first erected, from 1810 to 1865. Submersible dykes appeared then from
182 1862 to 1897. Finally, transverse structures as groynes and cross-beams were constructed between 1880
183 and 1908 (source: 1922 bathymetric map).

184 The study reach encompasses most of the reservoir of the Bourg-lès-Valence power plant facility
185 and extends over 9.8 km from kp 90.00 (acronym for kilometric point, which indicates the kilometric
186 distance from Lyon, with negative values upstream and positive downstream), 400 m upstream of the
187 confluence with the Doux River to kp 99.35, where the dam is located. The mean river width is 306 m
188 (range, 161–431 m) and the mean annual discharge is $1067 \text{ m}^3 \text{ s}^{-1}$. It was computed for the 1956–2013
189 period from the daily Rhône discharge at the Valence gauging station just downstream of the Isère
190 confluence from which we subtracted the daily Isère discharge at the Beaumont-Monteux gauging
191 station located just upstream of the confluence).



193 **Figure 1** - Location of the study reach in France (A), the Rhône basin (B) (1: Ternay gauging station,
 194 2: Beaumont-Monteux gauging station, 3: Valence gauging station), details of the local context (C),
 195 and description of the methodological combination used to characterize bed mobility in the study
 196 reservoir (D). **Pb affichage echelle à résoudre**

197
 198 The Bourg-lès-Valence power plant facility was put into service in 1968. The impounded reach,
 199 which is located along the study reach, stretches from kp 86.70 to kp 99.35 (diversion dam of la
 200 Roche-de-Glun; waterfall height = 11 m for the minimum bypassed discharge, see Figure 1C-D)
 201 (Institution interdépartementale des bassins Rhône-Saône, 2003). The artificial canal conveys most of
 202 the annual runoff to feed the Bourg-lès-Valence hydropower plant. The bypassed reach is divided into
 203 a short upstream section 1 km long (kp 98.30–99.35), corresponding to the downstream end of the
 204 reservoir, and an 8.5-km-long downstream section starting from the end of the reservoir (la Roche-de-
 205 Glun dam) (minimum discharge, 10–20 m³ s⁻¹ until 31/12/2014, 72 m³ s⁻¹ thereafter). One should note
 206 the presence of the Isère dam (Figure 1C), which is equipped with a dam and allows diversion of
 207 waters highly concentrated in suspended sediments from the headrace canal to the bypassed Rhône
 208 when a large flood of the Isère River occurs (Camenen et al., 2018). The power plant's capacity is
 209 2,200 m³ s⁻¹. When the power plant capacity is reached (e.g., 2,200 m³ s⁻¹), the bottom gates of the
 210 Roche-de-Glun dam are opened and excess discharge is diverted in the bypassed Rhône.



211
 212 **Figure 2** - Daily discharge in the study reach between 1968 and 2013 (corresponding to the daily
 213 discharge at the Valence gauging station just downstream of the Isère confluence from which we
 214 substrated the daily Isère discharge at the Beaumont-Monteux gauging station just upstream of the
 215 confluence, see Figure 1 for location) and sediment budget computation periods .

216
 217
 218

219 **3. Material and Methods**

220 We adopted a methodological strategy combining geomorphic and hydraulic approaches. First, we
221 characterized the morphological evolution of the study reach since the end of the 19th century by
222 comparing longitudinal profiles of the thalweg. Second, we assessed if the bedload transfer continuity
223 is still at least partially preserved by establishing sediment budgets in the reservoir and in the upstream
224 section of the bypassed reach. Finally, using a 1D hydraulic model, we estimated the current condition
225 of bed mobility by determining the competence of the river along the reservoir as well as the
226 maximum grain size exportable downstream.

227

228 **3.1 Bed vertical adjustment following channelization and impoundment**

229 The adjustment intensity following channelization (which occurred between 1862 and 1908) and
230 impoundment (1968) was determined by comparing longitudinal profiles of the thalweg from different
231 dates every 500 m (Parrot, 2015) between kp 90.00 and kp 99.00. The vertical evolution during the
232 first decades following channelization is not documented. Bathymetry was surveyed in 1897 and
233 between 1969 and 2009. For the earliest date, data were extracted from old bathymetric maps on
234 which thalweg elevation is indicated at least every 100 m and isolines with a resolution ranging from
235 0.20 m to 0.50 m are drawn. If information relative to the accuracy of these survey are unfortunately
236 not available, it seems reasonable to assume that is was lower than their resolution. For the 1969–2009
237 period, data come from surveys conducted by the CNR.

238

239 **3.2 Continuity of sediment transfer downstream the reservoir**

240 First, we computed a sediment budget in the reservoir between 1969, one year after the
241 commissioning of the hydropower plant, and 2011 (Figure 1 and Figure 2). The study reach
242 encompasses most of the reservoir until the dam (kp 90.90–99.20). Then, we computed a sediment
243 budget for the 1992-2013 period along the upstream section of the bypassed reach, from the dam to the
244 Isere confluence (kp 99.90-103.10). A recent inventory of authorized extractions indicates that gravel
245 was here intensively mined until 1992, with a removal of 1,409,000 m³ (+56,000 m³ possibly mined)
246 (Coeur, 2017). Extractions lowered sharply the bed and created three successive deep in-channel pits
247 (with a maximum deepening of 8 m, 11 m and 4.5 m from upstream to downstream) in which we
248 assume that most, or even all, of the bedload possibly passing the dam is trapped. It should thus allow
249 to estimate the bedload volume transported from the reservoir since 1992, if any.

250

251 **3.2.1 Data**

252 Bathymetric data were supplied by the CNR. They consist of points along cross sections 100 m
253 apart (Table 1). The mean point spacing along cross sections varies between 4.1 and 6.5 m. Data were
254 collected using a plumb line, a single-beam or a multi-beam sounder. The maximum measurement
255 error, given by the CNR, is respectively estimated between 0.1 and 0.4 m depending on date.

256 **Table 1** - Dates of bathymetric surveys and data characteristics.

Survey date	Reach	Device	Measurement error (m)	Mean number of points per cross section	Mean space between points (m)
1969	Reservoir	Plumb line	0.4	41.7	6.5
1992	Bypassed	Single-beam	0.2	24.1	8.4
2011	Reservoir	Multi-beam	0.1	46.3	5.9
2013	Bypassed	Multi-beam	0.1	49.4	4.1

257

258

259

3.2.2 Method

260

261

262

263

264

265

266

267

268

269

270

271

Sediment budget were obtained applying the method of Guertault et al. (2014) by computing area evolution along each cross section for successive dates and by longitudinally interpolating evolution area considering it as representative of changes that occurred between the mid-distance to the upstream cross section and the mid-distance to the downstream cross section. The budget is associated with a total error, composed of two terms: a measurement error and an interpolation error. It was computed applying the method developed by Arnaud et al. (2017). The measurement error was nevertheless determined as follows and not from repeated measurement of the same points at different dates where no change was assumed, as done for example by Brasington et al. (2000) or Gaeuman (2014): assuming a Gaussian distribution of the measurement error and approximating that the maximum error is equal to three times the standard deviation (σ), we estimated the measurement error (σ_{meas}) as the maximum error divided by 3.

272

3.3 Maximum grain size transported downstream of the reservoir: current functioning and optimization scenarios

273

274

275

276

277

278

279

280

281

282

283

284

Using a 1D hydraulic model implemented along the Rhône River from the Lake Geneva outlet to the delta (Dugué et al., 2015), we estimated for five different flood discharges the competence along the reservoir as well as the maximal grain size exportable downstream the dam. It was done for the current functioning of the reservoir but also for EmF scenarios aiming at maximizing the bedload transfer downstream of the reservoir (Table 2). For these optimisation scenarios, we increased the velocity in the reservoir by steepening the water slope along its whole course and/or we increased the discharge as much as possible in the bypassed section of the reservoir (Table 1). To this end, several combinations were tested by modifying at least one of the three following parameters that allow controlling the water elevation and the discharge in the different reaches of the facility: the maximum water elevation authorized in the bypassed section of the reservoir, the distribution of the discharge between the bypassed section and the headrace canal and the opening degree of the hydropower plant

285 gates. We finally retained two scenarios. The first one is characterised by a lowering of the maximum
 286 authorized water surface elevation at kp 98.30 (i.e. at the diversion), from 117.1 m for normal
 287 functioning to 114 m. For a 50 years return-interval flood, it decreases the waterfall height at the la
 288 Roche-de-Glun dam from 4.4 m for normal functioning to 0.7 m. The second scenario i) lowers the
 289 water surface elevation at kp 99.35 (i.e. at the Roche-de-Glun dam), from 116.8–117 m for normal
 290 functioning to 114 m, ii) derives most of the total discharge in the bypassed channel (keeping a
 291 residual flow of $100 \text{ m}^3 \text{ s}^{-1}$ in the headrace canal), iii) closes the gates of the power plant..

292
 293 **Table 2** - Synthesis of the three scenarios tested with the 1D hydraulic model (Q_r = Discharge in the
 294 reservoir).

Reservoir operating scenario	Water elevation (m)	Discharge at the headrace canal entrance ($\text{m}^3 \text{ s}^{-1}$)	Discharge in the bypassed channel ($\text{m}^3 \text{ s}^{-1}$)	Power plant gates
Normal functioning	117.1 at kp 98.3	2,000	$Q_r - 2,000$	Opened
	116.8-117 at kp 99.35			
EmF1	114 at kp 98.3	2,000	$Q_r - 2,000$	Opened
EmF2	114 at kp 99.35	100	$Q_r - 100$	Closed

295

296

297 3.3.1 Modelling parameters and simulated discharges

298 Running in "steady state" mode, the model was built with topo-bathymetric cross sections 100 m
 299 apart acquired by the CNR from 2004 to 2007. Inputs of tributaries were taken into account by
 300 assigning them a constant discharge equal to their mean annual discharge (Doux = $8.6 \text{ m}^3 \text{ s}^{-1}$; Isère =
 301 $329 \text{ m}^3 \text{ s}^{-1}$). The five simulated discharge values were chosen within a range from frequent to rare
 302 floods. They correspond to a return-interval (RI) at the Ternay gauging station equal to 2 ($3,200 \text{ m}^3 \text{ s}^{-1}$),
 303 5 ($3,900 \text{ m}^3 \text{ s}^{-1}$), 10 ($4,300 \text{ m}^3 \text{ s}^{-1}$), 20 ($4,700 \text{ m}^3 \text{ s}^{-1}$) and 50 ($5,200 \text{ m}^3 \text{ s}^{-1}$) years (Q_2 , Q_5 , Q_{10} , Q_{20}
 304 and Q_{50} respectively). The model predicts surface elevation and section-averaged velocity from which
 305 were computed local shear stress and competence at each node of each of the cross sections of the
 306 model.

307

308 3.3.2 Competence along the reservoir

309 For each simulated discharge and for each node of the model along each cross section, we
 310 determined the maximum sediment size that can be mobilized. In absence of any information
 311 regarding the bed state and structure, we provided two estimations of the competence, obtained with a
 312 critical Shields number of 0.03 and 0.06. The first one corresponds to a loose structure of the bed

313 surface, theoretically characterizing a high mobilization frequency of the bed material. The second one
 314 corresponds to a high degree of bed compaction, theoretically characterizing a low mobilization
 315 frequency of the bed material. The computation steps were the following.

316 We first computed the section-averaged total shear stress from the 1D model:

$$317 \quad \tau = \rho_w g R_h J \quad \text{Eq. 4}$$

318

319 where ρ_w is the water density (1000 kg m⁻³), g is the gravitational acceleration in m s⁻², R_h is the
 320 hydraulic radius in m, and J is the energy slope in m m⁻¹.

321

322 The section-averaged effective bed shear stress was then computed from the Meyer-Peter and
 323 Müller equation (1948):

$$324 \quad \tau'' = \tau \left(\frac{K}{K_s} \right)^{3/2} \quad \text{Eq. 5}$$

325 where K is the total Strickler coefficient in m^{1/3} s⁻¹, and K_s the skin Strickler coefficient (grain
 326 resistance) in m^{1/3} s⁻¹ was computed from the following equation:

$$327 \quad K_s = \frac{26}{D_{90}^{1/6}} \quad \text{Eq. 6}$$

328 where D_{90} is the size of bed material in millimetres for which 90% of the number of sediment clasts
 329 have a smaller size.

330

331 Then, we estimated for each node i of the model the local effective bed shear stress assuming a
 332 simple bed shear stress distribution based on the water depth, and assuming a homogeneous roughness
 333 throughout the river section (Camenen et al., 2011):

$$334 \quad \tau_i'' = \frac{H_i}{H} \tau'' \quad \text{Eq. 7}$$

335 where H_i is the water height in metres at node i of the cross section, and H the section-averaged water
 336 depth.

337

338 The competence at each node i was finally determined as follows:

339

$$340 \quad D_{\max(i)} = \frac{\tau_i''}{g \theta_{ci} (\rho_s - \rho_w)} \quad \text{Eq. 8}$$

341

342 where $D_{\max(i)}$ is the competence in i , in metres, θ_{ci} is the critical Shields number and ρ_s is the
 343 sediment density (2650 kg m⁻³).

344

345 Surface 90th grain size percentile (D_{90}) used in equation (6) was obtained from three volumetric
 346 samples taken in 2012 along the reservoir by Parrot (2015). Because grain size remains unknown

347 between samples (see Figure 1 for location of the samples), we had to use an estimate on most of cross
 348 sections. Two values were computed for each cross section. The first one (hereafter *G1*) was obtained
 349 by the linear interpolation between two consecutive samplings. For the second one (hereafter *G2*), the
 350 grain size at the location of each sample was used on a distance equal to half the distance to the next or
 351 the following sample.

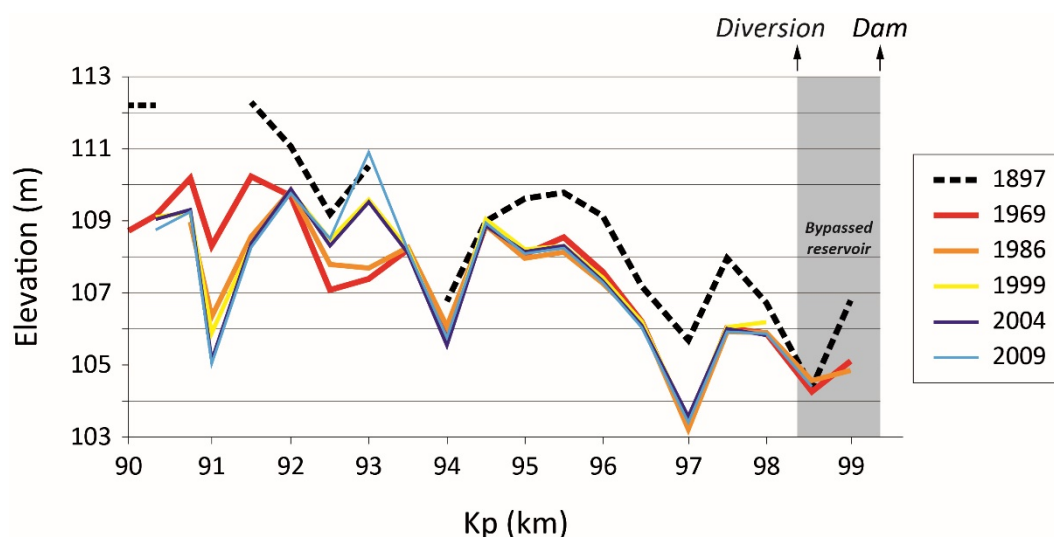
352

353

354 4. Results

355 4.1 Bed readjustment following channelization and impoundment

356 The comparison of the thalweg elevation from 1897 to 2009 clearly shows that most of the
 357 geomorphic changes along the study reach occurred following the first taming phase of the Rhône
 358 River (1862-1908), characterized by the channelization and the disconnection of its multi-thread bed
 359 channels (Figure 3). The incision induced by the channelization is probably underestimated since the
 360 first decades following it are not documented. Between 1897 and 1969, a large and widespread
 361 incision occurred, with a mean value of -1.67 m ($\sigma = 0.95$ m), equivalent to -0.021 m y^{-1} . From 1969
 362 to 2009, the bed stabilized downstream of kp 94.00, with a mean vertical evolution of -0.066 m ($\sigma =$
 363 0.14 m), equivalent to -0.0005 m y^{-1} . Along this section, the incision rate is 33 times lower than that
 364 of the 1897–1969 period. Upstream of kp 92.50, incision continued with a mean value of -1.64 m ($\sigma =$
 365 1.1 m), equivalent to -0.042 m y^{-1} . The incision occurred mainly before 1986. The section between kp
 366 92.50 and kp 93.50 underwent aggradation, very likely resulting from sediment reinjections (silt
 367 and/or sand) that occurred from 1984 to 2009 (five campaigns in 1984, 1997, 2000, 2001 and 2009).



368

369 **Figure 3** - Thalweg elevation every 500 m along the reservoir from 1897 to 2009. **Pb affichage ligne à**
 370 **résoudre**

371

372

373

374

375

4.3 Bedload transfer downstream of the reservoir

376

4.3.1 Sediment budget in the whole reservoir since dam completion

377

378

379

380

381

382

383

384

385

386

387

388

389

390

391

392

393

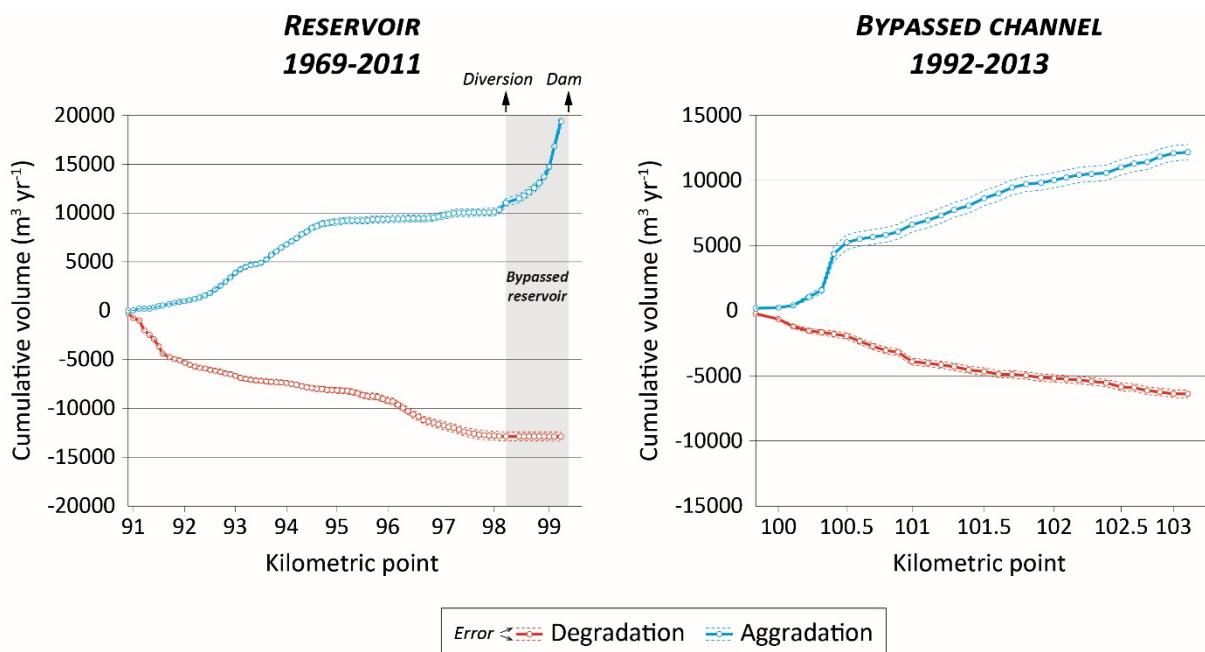
394

395

396

397

The sediment budget for the whole reservoir since dam completion is positive ($6,500 \text{ m}^3 \text{ y}^{-1}$ (± 800)), indicating that the bedload continuity could have been strongly, even totally, interrupted by the dam (Figure 4). Nevertheless, a large part of this deposited material is composed of fine sediments stored in the bypassed section of the reservoir (silt and sand) (Institution interdépartementale des bassins Rhône-Saône, 2003), which must not be taken into account in our budget. Deposition of a part of the suspended load can be explained by the fact that in the bypassed section of the reservoir i) the water slope strongly decreases (for a Q_2 , 0.19‰ upstream of the diversion, 0.017‰ downstream, i.e. a 11.2-fold decrease; for a Q_{50} , 0.36‰ upstream of the diversion, 0.26‰ downstream, i.e. a 1.4-fold decrease), ii) the bed in the downstream 500 m of the section undergoes a significant enlargement (twice that of upstream) with the bed 2.9 m wider than the dam, iii) the dam is located on the left side of the channel (Figure 5). This type of geometric configuration usually promotes lateral recirculation of flow with the eddy in the right half of the channel, contrary to the dam, and fine particle siltation. By excluding these fine sediment deposits, the budget for the entire reservoir would be negative with a value of $800 \text{ m}^3 \text{ y}^{-1}$ (± 300). Furthermore, because of dredging and sediment reinjection operations carried out at the end of the study period, a last modification must be applied to the budget by removing the corresponding volumes. In 2005, $29,000 \text{ m}^3$ were dredged in the center of the channel from kp 92.60 to kp 93.00. Since then, no deposit was observed in this area. In 2009, $37,500 \text{ m}^3$ of sandy material were reinjected along the outer bank between kp 92.50 and kp 93.50. At the time of the 2011 bathymetric survey, this stock was still in place. Once this taken in consideration, the budget amounts to $-1,000 \text{ m}^3 \text{ y}^{-1}$ (± 300). It induces thus that bedload transfer continuity from the reservoir to the bypassed channel is currently still at least partially preserved.



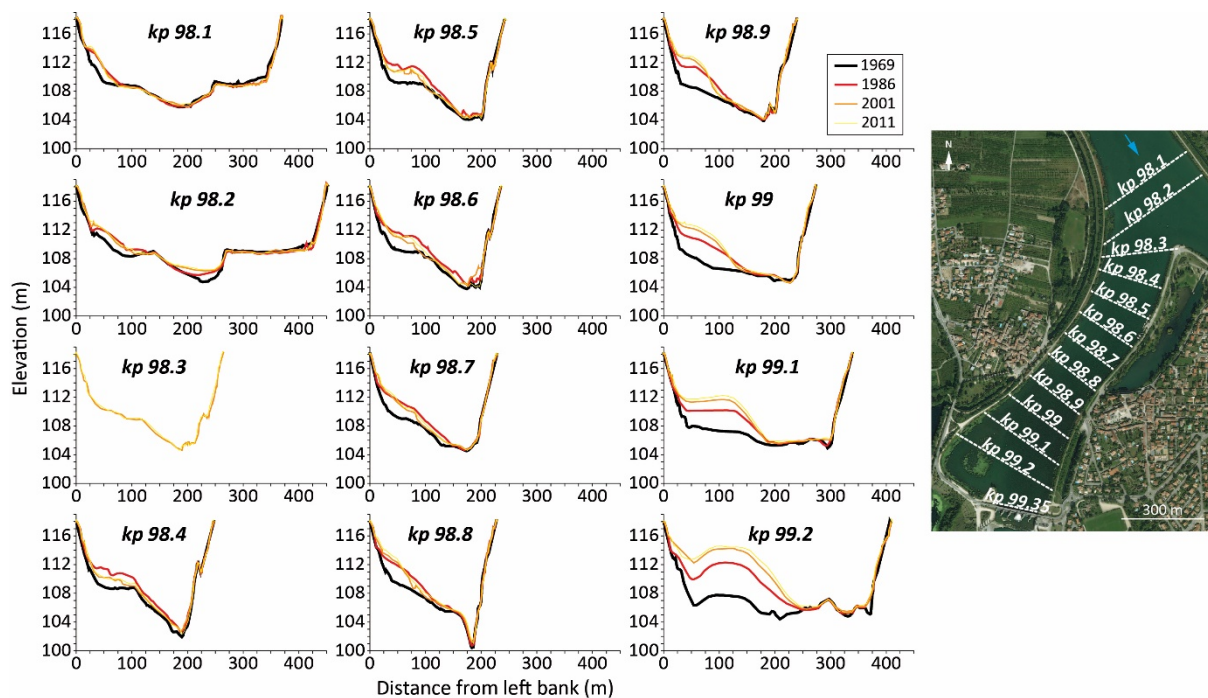
398

399 **Figure 4** - Net changes in cumulative aggraded and degraded volumes in a downstream direction over
 400 time. **Pb affichage ligne à résoudre**

401

402 Except for the bypassed section of the reservoir mentioned above, intensity of morphological
 403 changes decreased downstream, reflecting the increasing influence of the dam (Figure 4). An
 404 important part of the degradation took place upstream of kp 92.00. It was then quite low and regular
 405 until kp 94.50, from where it became almost null. Most of aggradation occurred upstream of kp 94.70,
 406 from which it became very low until the diversion.

407



408

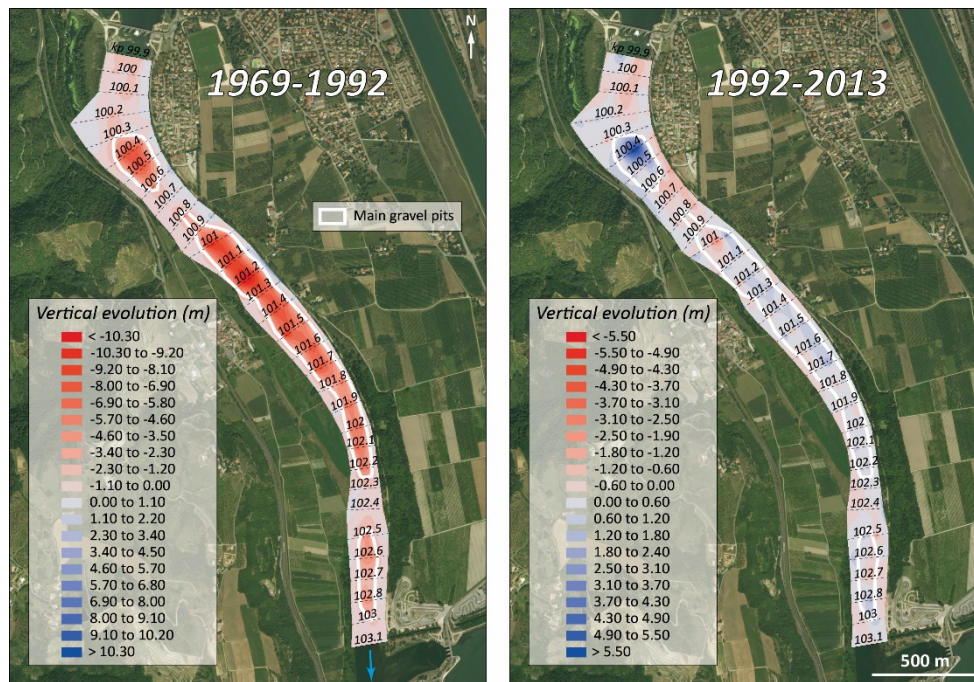
409 **Figure 5** - Insight of morphological evolution of the reservoir in its downstream bypassed section.

410

411 4.3.2 Sediment budget in the bypassed reach since 1992

412 More evidence of the preservation of the bedload transfer continuity is given by the morphological
 413 evolution downstream of the dam, along the upstream section of the bypassed channel (from the dam
 414 to the confluence with the Isère canal). Here the sediment budget between 1992 and 2013 is positive,
 415 with a value of $5,800 \text{ m}^3 \text{ y}^{-1} (\pm 600)$ (Figure 4 and Figure 6). It means that at least such volume were
 416 transported each year from the reservoir for this period. An important part of these sediments were
 417 deposited along the short upstream pit (kp 100.30-100.60) (Figure 4 and Figure 6).

418



419

420 **Figure 6** - Morphological evolution of the bypassed section downstream of the dam and upstream of
 421 the Isère confluence.

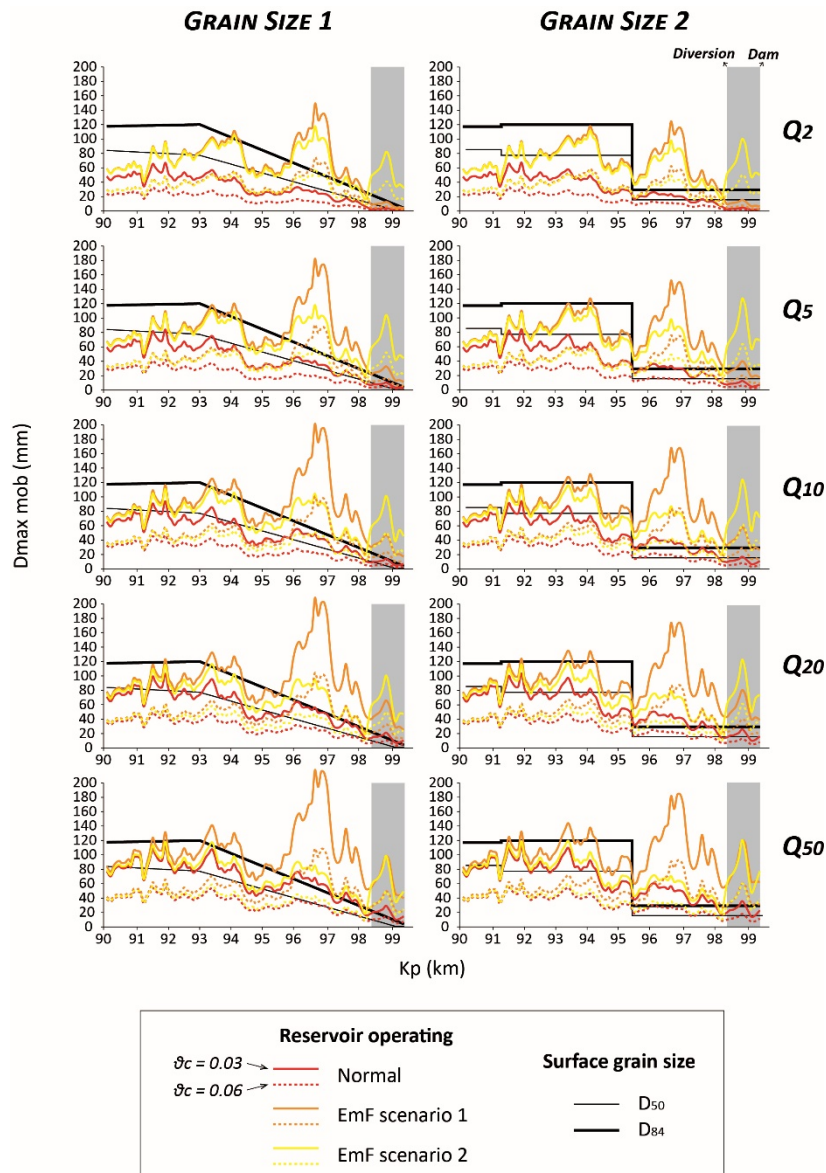
422

423 4.3.3 Maximum grain size exportable from the reservoir

424 *Current functioning*

425 For the whole reservoir length, and whatever the simulated discharge or the grain size considered,
 426 the maximum competence along each cross section decreases downstream, showing the clear
 427 longitudinal influence of the dam on bedload transport (Figure 7). Furthermore, the lowest value of the
 428 maximal competence is systematically located at kp 99.10. For a Q_2 , only very fine gravels (according
 429 to classification of Blott and Pye, 2001), at best, could be exported from the reservoir (2 mm at kp
 430 99.10 for a critical Shields number of 0.03 and for grain size G_2) (Figure 7). For a Q_{50} , the size
 431 increases to 14 mm, which belongs to medium gravel class (kp 99.10 for a critical Shields number of
 432 0.03 and for grain size G_2).

433



434

435 **Figure 7** - Longitudinal distribution of the maximum competence for the different GSD and
 436 discharges.

437

438 ***EmF conditions***

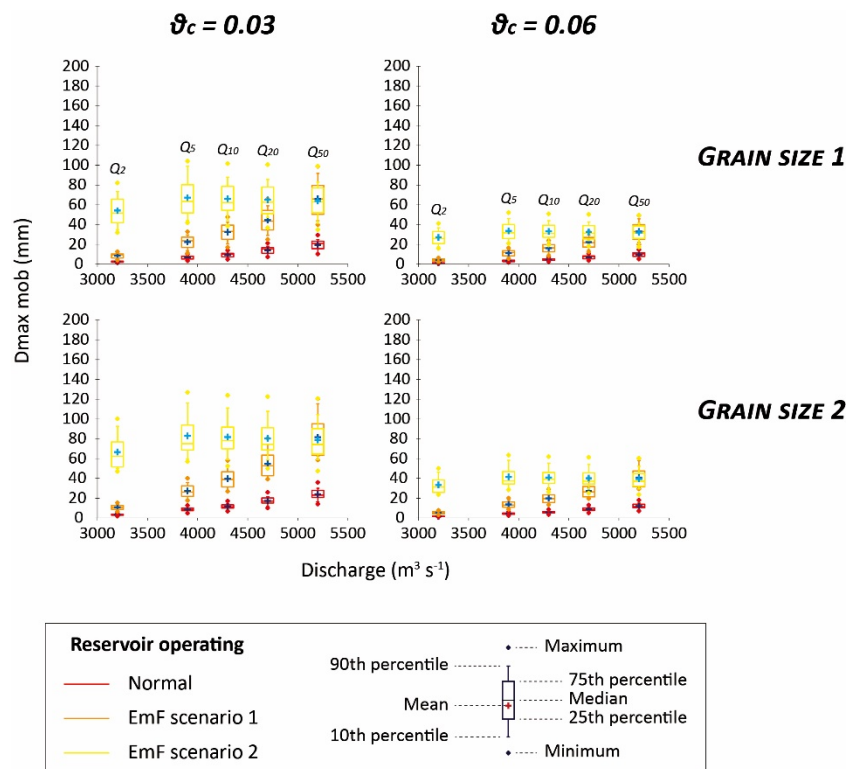
439 The effect of EmF is evident since the trend towards a downstream decrease of the competence
 440 observed in conditions of normal functioning tends to ease, even to disappear, at least up to kp 97.00
 441 (Figure 7). The attenuation of the trend is stronger for scenario 1 than for scenario 2 (Figure 7). For
 442 scenario 1, the stronger the discharge is, the stronger the attenuation is. Conversely, for scenario 2, the
 443 attenuation decreases when the discharge increases.

444 Upstream of the diversion, the best gain in maximum competence compared to normal functioning
 445 is obtained for scenario 1. Downstream of the diversion, scenario 2 would be the most efficient for all
 446 the simulated discharges except Q_{50} , for which the maximum competence is slightly higher for
 447 scenario 1 (Figure 7 and Figure 8). Moreover, the difference along this section between both scenarios

448 is little by little reduced when the discharge increases: while for scenario 1 the competence rises
 449 systematically, for scenario 2 it reaches a maximum for a Q_5 and then drops slightly (Figure 7 and
 450 Figure 8). Furthermore, the maximum competence for scenario 1 at Q_{50} and scenario 2 at Q_5 are
 451 almost the same.

452 For scenario 1, the lowest value of the maximal competence in the whole reservoir is located at kp
 453 99.30 whatever the grain size, except for a Q_{50} with grain size G_2 where it is located at kp 98.20, just
 454 upstream the diversion (Figure 7). Furthermore, it increases with discharge. For scenario 2, the lowest
 455 value of the maximal competence is systematically located at kp 98.20 (Figure 7). It increases until Q_5
 456 and then drops very slightly or remains almost constant.

457 Until a Q_5 , the maximal sediment size that could be exported from the reservoir is obtained with
 458 scenario 2 (Figure 7). For a Q_2 , it is equal to 18 mm (kp 98.20 for a critical Shields number of 0.03 and
 459 for grain size G_2), representing a nine fold increase compared to the normal functioning (2 mm). From
 460 Q_{10} , the maximal sediment size that could be exported from the reservoir is obtained with scenario 1
 461 (Figure 7). For a Q_{50} , it is equal to 56 mm at the best (kp 98.20 for a critical Shields number of 0.03
 462 and for grain size G_2), which is a fourfold increase compared to the normal functioning (14 mm).



463
 464 **Figure 8** - Box plots of the maximum competence for each of the 11 cross sections located along the
 465 bypassed section of the reservoir depending on the choice of the Shields parameter and GSD.

466

467

468 **5. Discussion**

469 **5.1 Bedload transfer in the reservoir**

470 The slight modifications that have occurred since the dam construction in 1968 (Figure 3) indicate
471 that the bed was almost totally adjusted to the conditions imposed by its previous channelization and
472 by the bedload supply decrease from tributaries and/or that the impoundment has inhibited the
473 possibilities for further adjustment. If the second factor played a role, we should expect a decrease
474 through time in the intensity of geomorphic changes in case of similar flood intensity and duration.
475 The comparison of degraded volumes between the two periods dominated by channel degradation
476 since 1969 (1969–1986 and 1999–2004) shows such a decrease despite comparable hydrological
477 conditions: for 1969–1986 and 1999–2004, there were respectively 15 and 10 days with discharge
478 higher than the 10-year RI discharge, which is the limit below which no significant changes in the
479 reservoir, especially degradation, could occur; and for each of both periods, one flood with a RI at
480 least equal to 35 years and at least one flood with a 10-year RI were counted (Dépret et al., 2018).
481 Furthermore, while degraded volumes for 1969–1986 were distributed quite linearly along the
482 reservoir, those for 1999–2004 diminished more and more downstream (Dépret et al., 2018). This
483 indicates that the study reach had still some potential for morphological changes at the time of dam
484 completion, even if most of the readjustments following channelization were probably already
485 realized, and that such potential was progressively reduced due to the impoundment.

486 Sediment budget downstream of the dam since 1992 indicates a bedload volume coming from the
487 reservoir at least equal to $5,800 \text{ m}^3 \text{ y}^{-1}$ (± 600). This value is 3.6 time higher than that given by Cortier
488 and Couvert (2001) ($1,600 \text{ m}^3 \text{ y}^{-1}$) and 19.7 times lower than their estimation of the annual bedload
489 before impoundment and channelization ($114,000 \text{ m}^3$). The situation could be greatly improved by
490 implementations of EmF since compared to a normal functioning of reservoir operating, the maximum
491 grain size that could be exported from the impoundment would increase from 2 cm to 18 cm for a Q_2
492 and from 14 cm to 56 cm for a Q_{50} .

493

494 **5.2 Implications for coarse sediment management in rivers influenced by run-of-river** 495 **dams**

496 On some of the bypassed reaches of the Rhône River, riprap removal, implying an increase of the
497 sediment supply to the river (Bravard and Gaydou, 2015), has been recently designed. The main goals
498 of these process-based restoration actions are to reactivate bedload transport and promote a shifting
499 riverscape mosaic to improve aquatic and riparian habitats. It raises the operational and scientific
500 questions of the degree of bedload transfer through a bypassed reach to its immediate downstream
501 reservoir, and then to the next bypassed reach. This will condition the spatial scale at which the
502 management of these sediment reinjections should be designed.

503 The present study shows that according to the most optimistic estimations, and in the absence of
504 EmF, the maximum grain size that could be exported from the reservoir would be smaller than coarse
505 gravels (according to the classification of Blott and Pye, 2001). It corresponds at the best to very fine
506 gravels (2 mm) for a Q_2 and to medium gravels for a Q_{50} (14 mm). In case of similar competence in

507 other reservoirs, it means that for the coarse fraction of the bedload, each Rhône River reach
508 composed of the succession of a bypassed section and its downstream reservoir should be considered
509 as almost independent of the surrounding ones. Depending on the grain size, bedload management
510 should therefore be considered at different spatial scales: very schematically, the reach scale for sizes
511 from fine gravels to boulders and the scale of the river corridor for very fine gravels and coarse sands.
512 Anticipating what could become the reinjected sediments therefore requires determining their grain
513 size as well as the longitudinal gradient of the competence from the restored bypassed reach to the
514 dam of the downstream reservoir.

515 So that habitat improvement can be beneficial at the largest spatial and temporal scales, promotion
516 of re-erosion or sediment augmentation must be done ideally on long bypassed reaches, with injection
517 in their upstream section. Nevertheless, because a large part of the bedload, if not all of it, should not
518 pass reservoirs, it could have potential future counter-effects that need to be considered (mainly
519 limitation for navigation and flood hazard aggravation). To make the existing human constraints and
520 the maximization of ecological benefits compatible, process-based solutions can then be implemented
521 jointly with gardening.

522 A more complex and elaborate way to manage bedload and to increase sediment transfer from
523 restored bypassed reaches would be the implementation of EmF using different configurations
524 depending on the discharge and the longitudinal location of dams in bypassed sections. For dams
525 located at diversions, and whatever the discharge, EmF similar to scenario 1 presented here (no
526 modification of the discharge distribution between the bypassed channel and the headrace canal)
527 should be preferred. For dams located downstream of the diversion, as for our study case, scenario 2
528 (almost no diversion of discharge in the headrace canal) seems more appropriate for relatively frequent
529 discharges (up to a maximum Q_5 – Q_{10}). This strategy should obviously be adjusted according to the
530 maximum grain size for which restoration of the continuity is planned. Broadly, these lessons
531 regarding the principles of bedload management learned from the present case study could be
532 generalized to similar rivers influenced by run-of-river dams presenting a strong and long-standing
533 bedload deficit and for which sediment replenishment is carried out.

534

535

536 **6. Conclusion**

537 This study aimed at estimating the potential for morphological adjustment of a run-of-river dam
538 impoundment, in which sediment augmentation was carried out, and for bedload transfer downstream.
539 Most of the geomorphic changes occurred before dam completion (1969) due to a decrease in coarse
540 sediment supply that occurred during the preceding 100 years because of channelization of the river
541 and less sediment delivery from tributaries. Since the reservoir's creation, changes are minor but the
542 bedload transfer is still maintained. Nevertheless, only particles up to medium-coarse gravels, at best,
543 can be exported downstream of the dam (2-3 mm for a Q_2 and 14-23 mm for a Q_{50}), which is less than

544 the bed D_{50} on most of the reservoir. Implementation of Ecomorphogenic Flows, here defined as
545 environmental flows whose objective is specifically to increase bedload transfer through the reservoir
546 to promote downstream habitat diversity, could improve the situation since the maximum grain size
547 exportable from the reservoir would increase strongly (a ninefold increase for a Q_2 , and around a
548 fourfold increase for discharges from a Q_5 to a Q_{50}).

549 Beyond the imperative need for trade-offs with other water uses if such a measure were
550 implemented, bedload management must be considered at the scale of the entire river corridor in order
551 to precisely localize and quantify the possible sources of sediment supply as well the conditions of
552 bedload transfer (competence and capacity). This characterization of the longitudinal bedload patterns,
553 as developed in Vazquez-Tarrio et al. (2018), can identify where a coarse sediment reinjection (by
554 gravel augmentation or by promoting lateral erosion through riprap removal) could be the most
555 sustainable and thus the most efficient. Finally, the use of an integrated and interdisciplinary
556 methodological approach (sediment budget, 1D model, surface-subsurface grain-size determination)
557 appears especially relevant since it increases the robustness of the results and potentially reduces
558 uncertainty.

559

560

561 **Acknowledgments**

562 This study was conducted within the Rhône Sediment Observatory (OSR), a multi-partner research
563 program funded through the Plan Rhône by the European Regional Development Fund (ERDF),
564 Agence de l'eau RMC, CNR, EDF and three regional councils (Auvergne-Rhône-Alpes, PACA and
565 Occitanie).

566

567

568 **References**

569 Anderson, D., Moggridge, H., Warren, P., Shucksmith, J., 2015. The impacts of ‘run-of-river’
570 hydropower on the physical and ecological condition of rivers. *Water Environ. J.* 29, 268-276.

571 Arnaud, F., Piégay, H., Béal, D., Collery, P., Vaudor, L., Rollet, A.J., 2017. Monitoring gravel
572 augmentation in a large regulated river and implications for process-based restoration. *Earth*
573 *Surf. Process. Landforms* 42 (13), 2147-2166.

574 Astrade, L., Jacob-Rousseau, N., Bravard, J.P., Allignol, F., Simac, L., 2011. Detailed chronology of
575 mid-altitude fluvial system response to changing climate and societies at the end of the Little Ice
576 Age (Southwestern Alps and Cévennes, France). *Geomorphology* 133, 100-116.

577 Beechie, T.J., Sear, D.A., Olden, J.D., Pess, G.R., Buffington, J.M., Moir, H., Roni, P., Pollock, M.M.,
578 2010. Process-based principles for restoring river ecosystems. *Bioscience* 60 (3), 209-222.

579 Bednarek, A.T., 2001. Undamming Rivers: A review of the ecological impacts of dam removal.
580 *Environ. Manag.* 27 (6), 803-814.

- 581 Bieri, M., Muller, M., Boillat, J.L., Schleiss, A.J., 2012. Modeling of sediment management for the
582 Lavey run-of-river HPP in Switzerland. *Journal of Hydraulic Engineering* 138 (4), 340-347.
- 583 Bizzi, S., Dinh, Q., Bernardi, D., Denaro, S., Schippa, L., Soncini-Sessa, R., 2015. On the control of
584 riverbed incision induced by run-of-river power plant. *Water Resour. Res.* 51, 5023-5040.
- 585 Blott, S.J., Pye, K., 2001. GRADISTAT: A grain size distribution and statistics package for the
586 analysis of unconsolidated sediments. *Earth Surf. Process. Landforms* 26, 1237-1248.
- 587 Brandt, S.A., 2000. Classification of geomorphological effects downstream of dams. *Catena* 40, 375-
588 401.
- 589 Brasington, J., Langham, J., Rumsby, B., 2003. Monitoring and modelling morphological change in a
590 braided gravel-bed river using high resolution GPS-based survey. *Earth Surf. Process.*
591 *Landforms* 25, 973-990.
- 592 Bravard, J.P., 1987. *Le Rhône, du Léman à Lyon*. La Manufacture, Lyon.
- 593 Bravard, J.P., 2002. Les réponses des systèmes fluviaux à une réduction des flux d'eau et de sédiments
594 sous l'effet du reboisement en montagne. *La Houille Blanche* 3, 68-71.
- 595 Bravard, J.P., 2010. Discontinuities in braided patterns: The River Rhône from Geneva to the
596 Camargue delta before river training. *Geomorphology* 117 (3-4), 219-233.
- 597 Bravard, J.P., Gaydou, P., 2015. Historical development and integrated management of the Rhône
598 River floodplain, from the Alps to the Camargue delta, France, in: Hudson, P.F., Middelkoop, H.
599 (Eds.), *Geomorphic approaches to integrated floodplain management of lowland fluvial systems*
600 *in North America and Europe*. Springer, New York, pp. 289-320.
- 601 Bravard, J.P., Landon, N., Peiry, J.L., Piégay, H., 1999b. Principles of engineering geomorphology for
602 managing channel erosion and bedload transport, examples from French rivers. *Geomorphology*
603 31, 291-311.
- 604 Bravard, J.P., Peiry, J.L., 1993. La disparition du tressage fluvial dans les Alpes françaises sous l'effet
605 de l'aménagement des cours d'eau (19-20ème siècle). *Z. Geomorphol., Suppl.-Bd.* 88, 67-79.
- 606 Camenen, B., Holubová, K., Lukac, M., Le Coz, J., Paquier, A., 2011. Assessment of methods used in
607 1D models for computing bed-load transport in a large river: the Danube River in Slovakia. *J.*
608 *Hydraulic Eng.*, 137, 1190-1199.
- 609 Camenen, B., Naudet, G., Dramais, G., Paquier, A., & Le Coz, J., 2018. Evaluation of the sand
610 dynamics at the Isère-Rhône confluence, France. *Sci. Total Environ.*, this issue.
- 611 Cœur, D., 2017. Etude historique des prélèvements de sédiments dans le Rhône, 1954-2010. Report +
612 annexes.
- 613 Cortier, B., Couvert, B., 2001. Causes et conséquences du blocage actuel de la dynamique fluviale et
614 du transit sédimentaire du Rhône. *La Houille Blanche* 8, 72-78.
- 615 Costigan, K.H., Ruffing, C.M., Perkin, J.S., Daniels, M.D., 2016. Rapid response of a sand-dominated
616 river to installation and removal of a temporary run-of-the-river dam. *River Res. Applic.* 32,
617 110-124.

- 618 Csiki, S., Rhoads, B.L., 2010. Hydraulic and geomorphological effects of run-of-river dams. *Progr.*
619 *Phys. Geogr.* 34 (6), 755-780.
- 620 Csiki, S., Rhoads, B.L., 2014. Influence of four run-of-river dams on channel morphology and
621 sediment characteristics in Illinois, USA. *Geomorphology* 206, 215-229.
- 622 Curtis, K.E., Renshaw, C.E., Magilligan, F.J., Dade, W.B., 2010. Temporal and spatial scales of
623 geomorphic adjustments to reduced competency following flow regulation in bedload-
624 dominated systems. *Geomorphology* 118, 105-117.
- 625 Dade, W.B., Renshaw, C.E., Magilligan, F.J., 2011. Sediment transport constraints on river response
626 to regulation. *Geomorphology* 126, 245-251.
- 627 Dépret, T., Piégay, H., Dugué, V., Noirot, B., Faure, J.B., Le Coz, J., Camenen, B., Cassel, M.,
628 Bultingaire, L., Yousefi, S., Michel K., 2018. Mesures et modélisations du fonctionnement
629 hydrosédimentaire du secteur de Bourg-lès-Valence – Final synthesis report, OSR4.
- 630 Dessaix, J., Fruget, J.F., Olivier, J.M., Beffy, J.L., 1995. Changes of the macroinvertebrate
631 communities in the dammed and by-passed sections of the French upper Rhône after regulation.
632 *River Res. Applic.* 10, 265-279.
- 633 Dugué, V., Walter, C., Andries, E., Launay, M., Le Coz, J., Camenen, B., Faure, J.-B. 2015.
634 Accounting for hydropower schemes' operation rules in the 1D hydrodynamic modeling of the
635 Rhône River from lake Genova to the Mediterranean sea. *Proceedings (E-proceedings)*, 36th
636 IAHR Congress, 28 June - 3 July, The Hague, The Netherlands. 9 p.
- 637 Fencel, J.S., Mather, M.E., Costigan, K.H., Daniels, M.D., 2015. How big of an effect do small dams
638 have? Using geomorphological footprints to quantify spatial impact of low-head dams and
639 identify patterns of across-dam Variation. *PLoS ONE*, 10(11): e0141210.
640 doi:10.1371/journal.pone.0141210.
- 641 Gaeuman, D. 2012. Mitigating downstream effects of dams, in: Church, M., Biron, P., Roy, AG.
642 (Eds.), *Gravel-bed rivers: Processes, tools, environments*. John Wiley & Sons, Chichester, pp.
643 182-189.
- 644 Gaeuman, D., 2014. High-flow gravel injection for constructing designed in-channel features. *River*
645 *Res. Applic.* 30, 685-706.
- 646 Graf, W.L., 2006. Downstream hydrologic and geomorphic effects of large dams on American rivers.
647 *Geomorphology* 79, 336-360.
- 648 Grant, G.E., 2012. The Geomorphic response of gravel-bed rivers to dams: Perspectives and prospect,
649 in: Church, M., Biron, P., Roy, AG. (Eds.), *Gravel-bed rivers: Processes, tools, environments*.
650 John Wiley & Sons, Chichester, pp. 165-181.
- 651 Guertault, L., Camenen, B., Peteuil, C., Paquier, A., 2014. Long term evolution of a dam reservoir
652 subjected to regular flushing events. *Adv. in Geosci.* 39, 89-94.
- 653 Ibisate, A., Diaz, E., Ollero, A., Acin, V., 2013. Channel response to multiple damming in a
654 meandering river, middle and lower Aragon River (Spain). *Hydrobiologia* 712, 5-23.

- 655 Institution interdépartementale des bassins Rhône-Saône, 2003. Etude globale pour une stratégie de
656 réduction des risques dus aux crues du Rhône : 1998-2003.
- 657 Isaac, N., Eldho, T.I., 2016. Sediment management studies of a run-of-the river hydroelectric project
658 using numerical and physical model simulations. *Intern. J. River Basin Manag.* 14 (2), 165-175.
- 659 Jones, J.I., Murphy, J.F., Collins, A.L., Sear, D.A., Naden, P.S., Armitage, P.D., 2012. The impact of
660 fine sediment on macro-invertebrates. *River Res. Applic.* 1055-1071.
- 661 Kibler, K.M., Tullos, D.D., Kondolf, G.M., 2011. Learning from dam removal monitoring: Challenges
662 to selecting experimental design and establishing significance of outcomes. *River Res. Applic.*
663 27, 967-975.
- 664 Kibler, K.M., Tullos, D.D., 2013. Cumulative biophysical impact of small and large hydropower
665 development in Nu River, China. *Water Resour. Res.* 49, 3104-3118, doi:10.1002/wrcr.20243.
- 666 Kondolf, G.M., Gao, Y., Annandale, G.W., Morris, G.L., Jiang, E., Zhang, J., Cao, Y., Carling, P., FU,
667 K., Guo, Q., Hotchkiss, R., Peteuil, C., Sumi, T., Wang, H.W., Wang, Z., Wei, Z., Wu, B., Wu,
668 C., Yang, C.T., 2014. Sustainable sediment management in reservoirs and regulated rivers:
669 Experiences from five continents, *Earth's Future* 2, 256-280, doi:10.1002/2013EF000184.
- 670 Kostic, S., Parker, G., 2003. Progradational sand-mud deltas in lakes and reservoirs. Part 1. Theory
671 and numerical modeling. *J. Hydraul. Res.* 41 (2), 127-140.
- 672 Lajczak, A., 1996. Modelling the long-term course of non-flushed reservoir sedimentation and
673 estimating the life of dams. *Earth Surf. Process. Landforms* 21, 1091-1107.
- 674 Lefort, P., Chapuis, M., 2012. Incidence des aménagements hydro-électriques sur la morphologie des
675 tronçons court-circuités de la Durance et du Verdon. *La Houille Blanche* 2, 42-48
- 676 Liébault, F., Clément, P., Piégay, H., Landon, N., 1999. Assessment of bedload delivery from
677 tributaries: The Drôme River case, France. *Arct., Antarct., Alp. Res.* 31 (1), 108-117.
- 678 Liébault, F., Clément, P., Piégay, H., Rogers, C.F., Kondolf, G.M., Landon, N., 2002. Contemporary
679 channel changes in the Eygues basin, southern French Prealps: the relationship of subbasin
680 variability to watershed characteristics. *Geomorphology* 45 (1-2), 53-66.
- 681 Liébault, F., Piégay, H., 2002. Causes of 20th century channel narrowing in mountain and piedmont
682 rivers of southeastern France. *Earth Surf. Process. Landforms* 27, 425-444.
- 683 Lobrera, G., Munoz, I., Lopez-Tarazon, J.A., Verciat, D., Batalla, R.J., 2016. Effects of flow
684 regulation on river bed dynamics and invertebrate communities in a Mediterranean river.
685 *Hydrobiologia* 784 (1), 283-304.
- 686 Magilligan, F.J., Graber, B.E., Nislow, K.H., Chipman, J.W., Sneddon, C.S., Fox, C.A., 2016. River
687 restoration by dam removal: Enhancing connectivity at watershed scales. *Elementa: Science of*
688 *the Anthropocene* 4, 000108, doi: 10.12952/journal.elementa.000108.
- 689 Malavoi, J.R., Garnier, C.C., Landon, N., Recking, A., Baran, P., 2011. Eléments de connaissance
690 pour la gestion du transport solide en rivière. ONEMA, 215 pp.

- 691 McManamay, R.A., Oigbokie, C.O., Kao, S.C., Bevelhimer, M.S., 2016. Classification of US
692 hydropower dams by their modes of operation. *River Res. Applic.* 32, 1450-1468.
- 693 Meyer-Peter, E., Müller, R., 1948. Formulas for bed load transport. Proceedings, 3rd Meeting of
694 International Association Hydraulic Resources, Stockholm, pp. 39-64.
- 695 Morris, G.L., Annandale, G., Hotchkiss, R., 2008. Reservoir Sedimentation, in: Garcia, M. (Eds.),
696 Sedimentation engineering: Processes, measurements, modeling, and practice. American
697 Society of Civil Engineers Manual 110, pp. 579-612.
- 698 Morris, G.L., Fan, J., 1998. Reservoir sedimentation handbook: Design and management of dams,
699 reservoirs, and watersheds for sustainable use. McGraw-Hill Book Co., New York.
- 700 Nilsson, C., Berggren, K., 2000. Alterations of Riparian Ecosystems Caused by River Regulation.
701 *BioScience* 50 (9), 783-792.
- 702 Olivier, J. M., Carrel, G., Lamouroux, N., Dole-Olivier, M.J., Malard, F., Bravard, J.P. Amoros, C.,
703 2009. The Rhône river basin. In: Robinson, C., Uehlinger, U., Tockner, K. (Eds.), *Rivers of*
704 *Europe*. Elsevier, San Diego, pp. 247-295.
- 705 Parrot, E., 2015. Analyse spatio-temporelle de la morphologie du chenal du Rhône du Léman à la
706 Méditerranée. Ph.D. Thesis, Lyon 3 University.
- 707 Pearson, A.J., Pizzuto, J., 2015. Bedload transport over run-of-river dams, Delaware, U.S.A.
708 *Geomorphology* 248, 382-395.
- 709 Petts, G.P., Gurnell, A.M., 2005. Dams and geomorphology: Research progress and future directions.
710 *Geomorphology* 71, 27-47.
- 711 Petts, G.P., Gurnell, A. 2013. Hydrogeomorphic effects of reservoirs, dams, and diversions, in:
712 Shroder J. (Editor in Chief), Wohl, E. (Eds.), *Treatise on Geomorphology*. Academic Press, San
713 Diego CA. Vol. 13, *Fluvial Geomorphology*, pp. 96-113.
- 714 Poff, N.L., 2017. Beyond the natural flow regime? Broadening the hydro-ecological foundation to
715 meet environmental flows challenges in a non-stationary world. *Freshwater Biology*, doi:
716 10.1111/fwb.13038.
- 717 Poff, N.L., Tharme, R.E., Arthington, A.H., 2017. Evolution of environmental flows assessment
718 science, principles, and methodologies, in: Horne, A.C., Webb, J.A., Stewardson, M.J., Richter,
719 B., Acreman, M. (Eds.), *Water for the environment, from policy and science to implementation*
720 *and management*. Academic Press, pp. 203-236.
- 721 Poff, N.L., Zimmerman, J.K.H., 2010. Ecological responses to altered flow regimes: a literature
722 review to inform the science and management of environmental flows. *Freshwater Biology* 55,
723 194-205.
- 724 Poinsart, D., 1992. Effets des aménagements fluviaux sur les débits liquides et solides. L'exemple du
725 Rhône dans les plaines de Miribel-Jonage et Donzère-Mondragon. Ph.D. Thesis, Lyon 3
726 University.

- 727 Poinsart, D., Salvador, P.G., 1993. Histoire de l'endiguement du Rhône à l'aval de Lyon (XIXe
728 siècle). Actes du colloques "Le fleuve et ses métamorphoses", Lyon, France, 13-15 mai 1992,
729 pp. 299-313.
- 730 Rheinheimer D.E., Yarnell, S.M., 2017. Tools for sediment management in rivers, in: Horne, A.C.,
731 Webb, J.A., Stewardson, M.J., Richter, B., Acreman, M. (Eds.), Water for the environment,
732 from policy and science to implementation and management. Academic Press, pp. 237-263.
- 733 Rollet, A.J., Piégay, H., Dufour, S., Bornette, G., Persat, H., 2013. Assessment of consequences of
734 sediment deficit on a gravel river bed downstream of dams in restoration perspectives:
735 Application of multicriteria, hierarchical and spatially explicit diagnosis. *River Res. Applic.* 30
736 (8), 939-953.
- 737 Rolls, R.J., Bond, N.R., 2017. Environmental and ecological effects of flow alteration in surface Water
738 ecosystems, in: Horne, A.C., Webb, J.A., Stewardson, M.J., Richter, B., Acreman, M. (Eds.),
739 Water for the environment, from policy and science to implementation and management.
740 Academic Press, pp. 237-263.
- 741 Rosenberg, D.M., McCully, P., Pringle, C.M., 2000. Global-scale environmental effects of
742 hydrological alterations: Introduction. *Bioscience* 50 (9), 746-751.
- 743 Schmidt, J.C., Wilcock, P.R., 2008. Metrics for assessing the downstream effects of dams. *Water*
744 *Resour. Res.* 44, W04404, doi:10.1029/2006WR005092.
- 745 Sindelar, C., Schobesberger, J., Habersack, H., 2017. Effects of weir height and reservoir widening on
746 sediment continuity at run-of-river hydropower plants in gravel bed rivers. *Geomorphology* 91,
747 106-115.
- 748 Snyder, N.P., Rubin, D.M., Alpers, C.N., Childs, J.R., Curtis, J.A., Flint, L.E., Wright, S.A., 2004.
749 Estimating accumulation rates and physical properties of sediment behind a dam: Englebright
750 Lake, Yuba River, northern California. *Water Resour. Res.* 40, W11301,
751 doi:10.1029/2004WR003279.
- 752 Stroffek, S., Amoros, C., Zylberblat, M., 1996. La logique de réhabilitation physique appliquée à un
753 grand fleuve : le Rhône. *Géocarrefour* 71 (4), 287-296.
- 754 Vazquez-Tarrío, D., Tal, M., Camenen, B., Piégay, H., 2018. Present-day bed load transport capacities
755 along the Rhône River following a century and half of human modifications. *Sci. Total*
756 *Environ.*, this issue.
- 757 Warner, R.F., 2000. Gross channel changes along the Durance River, Southern France, over the last
758 100 years using cartographic data. *River Res. Applic.* 16, 141-157.
- 759 Williams, G.P., Wolman, M.G., 1984. Downstream effects of dams on alluvial rivers. United States
760 Geological Survey Professional Paper 1286.
- 761 Yarnell, S.M., Mount, J.F., Larsen, E.W., 2006. The influence of relative sediment supply on riverine
762 habitat heterogeneity. *Geomorphology* 80, 310-324.